Desalination and Water Treatment
www.deswater.com
18 (2010) 257–263
June
1944-3994 / 1944-3986 © 2010 Desalination Publications. All rights reserved.
doi: 10.5004/dwt.2010.1782

A new approach to the characterization of reverse osmosis membrane by dynamic hysteresis

Eunsu Lee, Sangyoup Lee, Seungkwan Hong*

Department of Civil, Environmental & Architectural Engineering, Korea University, 1, 5-ka, Anam-Dong, Sungbuk-Gu, Seoul 136-713, Republic of Korea
email: skhong21@korea.ac.kr

Received 31 May 2009; Accepted 18 December 2009

ABSTRACT

Physical aspects of dynamic hysteresis for characterizing reverse osmosis (RO) membranes have been investigated. Dynamic hysteresis was used as a parameter of showing physical surface characteristics of RO membranes. Automated microbalance was utilized to determine dynamic hysteresis based on the Wilhelmy plate method. Dynamic hysteresis determined with non-polar liquid was related to physical surface characteristics including surface roughness and heterogeneity determined by atomic force microscopy imaging and analysis. A remarkable correlation between dynamic hysteresis and surface heterogeneity was obtained when non-polar liquid was used during the measurements. Dynamic hysteresis increased as the surface heterogeneity of RO membrane increased.

Keywords: Membrane characterization; Dynamic hysteresis; RO membrane; Physical surface characteristics

1. Introduction

Reverse osmosis (RO) membranes are currently being used in a wide range of applications, including brackish/seawater desalination, drinking water treatment, and wastewater reuse. Efficient application of RO membranes in various water treatments is often limited due to membrane fouling. In case of RO membranes, membrane fouling is surface phenomenon as RO membranes are considered to be non-porous. Therefore, surface characteristics of RO membranes are one of the key factors affecting membrane fouling. In addition, other factors affecting membrane fouling such as foulant characteristics and feed water solution chemistry are rather natural factors with having difficulty in handling. With these reasons, there have been various efforts to elucidate the relationship between the surface characteristics of RO membrane and the extent of membrane fouling [1–7]. Consequently, there has been a great improvement in membrane fabrication technology, especially in surface modification, where membrane surface properties have been tailored toward reducing membrane fouling as well as enhancing permeation [8–13].

Surface property of RO membranes affecting membrane fouling includes both chemical and physical characteristics. The latter most includes surface roughness commonly determined by image analysis using atomic force microscopy (AFM). In addition, morphological surface heterogeneity (i.e., heterogeneity in the distribution of peak and valley structures) belongs to physical surface characteristics [14]. Based on these surface characteristics and their relation to membrane fouling, it has been known that membranes with less

*Corresponding author.

rough surface are favorable to reducing membrane fouling caused by particulate and organic matters [1,3,4,7,15–17]. In practical point of view, however, these characterization methods are time and money consuming because the equipments are hard to manipulate and expensive. Furthermore, hydrophobicity, roughness, and heterogeneity are showing difficulty in interrelating experimental data obtained from each measurement. Therefore, developing simple and reliable techniques to determine membrane surface characteristics is of paramount importance in membrane fouling study.

With this goal, surface characterization based on dynamic hysteresis analysis was investigated. In this study, dynamic hysteresis was adopted to determine various surface characteristics of RO membranes, and the hysteresis data were physical surface characteristics including surface roughness, morphological heterogeneity, and hydrophobicity. Based on the results obtained in this study, it is expected that the surface characteristics of RO membranes determined by the dynamic hysteresis analysis are informative for further investigation on the relationship between dynamic hysteresis and membrane fouling.

2. Material and methods

2.1. Reverse osmosis membranes

Four commercial seawater RO membranes were used. The RO membranes were RE-8040 (WJ chemical), SW-30HR (Dow chemical), TM-820 (Toray), and SWC-5 (Hydranautics). All membranes were polyamide thin film composite (TFC) membranes with an average salt rejection over 99.5%. General property of the membranes in terms of contact angle and surface roughness was determined and listed in Table 1. The membranes were immersed in deionized (DI) water at 4°C with water replaced regularly. Prior to each analysis, the membranes were put into 25°C DI water for 2 h as all the instrumental analyses in this study were carried out at 25°C.

Table 1
Average concentration of heavy metals in the infiltration splash block and rain garden (Feb. 2008).

Membrane	Contact angle (°)	Roughness (nm)
TM-820	79.0	77.5
RE-8040	73.6	82.1
SWC-5	72.4	127.4
SW-30HR	24.0	87.3

2.2. Mica sheet

Mica sheet is a layered aluminosilicate mineral having one intrinsic negative surface charge per 48 Å^2. This is because of isomorphous substitution of aluminium for silicon. Unlike glass, mica sheet does not have any surface silanol groups. Instead, high negative mica charge provides an electrostatic anchoring of cationic surfactants which can be utilized for modifying the mica sheet surface.

2.3. Solution chemistry

Non-polar (i.e., diiodomethane) liquids were used as test solutions during the hysteresis measurements. In case of using the non-polar liquid, the dynamic hysteresis data were related to the physical surface characteristics such as surface roughness and heterogeneity. When relating the dynamic hysteresis data to other surface characteristics, the same solution chemistry was employed for direct comparison. Solution pH was varied as needed using 0.1 M HCl or NaOH stock solutions. Solution TDS was adjusted using NaCl.

2.4. Dynamic hysteresis

Dynamic hysteresis was determined based on the Wilhelmy plate method [18–23]. During the measurement, a membrane sample was held by the automated microbalance, then pushed into or pulled from a test liquid. Therefore, the measured force acting on the membrane sample alternates depending on direction of the movement. The force acting on the membrane sample when pushing into the test liquid is the advancing force (F_A), while pulling from the test liquid is the receding force (F_R). These advancing and receding forces are defined as Eqs. (1) and (2), respectively [24,25].

$$F_A = W + P\gamma \cos \theta_A \quad (1)$$

$$F_R = W + P\gamma \cos \theta_R - B \quad (2)$$

where, W is the weight of membrane sample, P the perimeter of membrane sample, g the surface tension of test liquid; q_A and q_R the advancing and receding contact angles between test liquid and membrane sample, respectively, and B the buoyancy force. Since the instrument automatically tares the weight of membrane sample the effect of the buoyancy force can be eliminated by extrapolating the graph back to zero depth of immersion. The difference between the receding and advancing forces can be defined as dynamic hysteresis as expressed in Eq. (3) [21,26–28].

$$\text{Dynamic hysteresis} = \frac{F_A}{P} - \frac{F_R}{P} \quad (3)$$

Table 2
Experimental parameters for dynamic hysteresis measurements.

Parameter	Value
Speed up (mm/min)	5.0
Speed down (mm/min)	5.0
Wait when up (s)	0
Wait when down (s)	0
Start depth (mm)	2.0
Immersion depth (mm)	10.0
Ignore first (mm)	2.0
Return position (mm)	4.0
Reset speed (mm/min)	40.0
Sample interval (s)	5.0
Detect range (mN/m)	5.0
Number of repeat	5

Here, the measured F is divided by membrane sample perimeter (P) to express the dynamic hysteresis as force per unit length (F/L, mN/m) [28]. In graphical analysis, the dynamic hysteresis is the vertical width between parallel advancing and receding force lines in F/L (y axis) versus moving distance (x axis) relationship [28].

The measurements were carried out using a Sigma 701 microbalance (KSV Instrument, Ltd., Finland) interfaced with a PC for automatic control and data acquisition. It was operated by holding a membrane sample attached to microbalance vertically. A liquid cell containing a test liquid moved up and down at constant speed rate repeatedly during the measurements. All parameters employed during the hysteresis measurements are listed in Table 2. The surface tension of test liquids was measured at each time by the Force Du Nouy ring method at 25°C [28]. The ring was rinsed by ethyl alcohol prior to the measurement. More details on the way of using the instrument were described well previously [28].

2.5. Contact angle

Contact angle measurements were performed with a goniometer (DM 500, Kyowa Interface Science, Japan). Equilibrium contact angle measurements as described by Marmur [29] were adopted. Equilibrium contact angle was the average of the left and right contact angles. Ten measurements for each membrane were performed. The reported values are the average of 10 equilibrium contact angles.

2.6. Surface roughness and heterogeneity

Membrane surface roughness was analyzed by AFM imaging (PUCOStation AFM, Surface Imaging Systems, Herzogenrath, Germany). Liquid phase AFM imaging was conducted in contact mode with silicon probes of which backside had 30-nm thick aluminum reflex coating for better resolution and stability in liquid phase applications (APPNANO, Applied Nano Structures, Inc., Santa Clara, CA). The probe has a spring constant of 0.1 N/m (±0.08 N/m), resonance frequency of 28 kHz (±10 kHz), tip radius of 5–6 nm, tip height of 14 μm (±2 μm), and cantilever length of 225 μm (±10 μm). The RO membranes were immersed in a liquid cell containing pre-adjusted test solution in terms of pH and TDS.

All membranes were scanned three times with randomly selecting a scan position. Membranes surface roughness was quantified by root mean square (RMS) roughness, which is the RMS deviation of the peaks and valleys from the mean plane. Approaching force ranged from 4.0 to 6.0 N/m with a scan speed of 0.7 line/s and scan area of 10×10 μm^2. Scanned images were analyzed using SPIP software (Surface Imaging Systems, Herzogenrath, Germany). Each image was flattened by a baseline prior to roughness analyses. In addition, surface morphological heterogeneity was determined from scanned images by calculating the density of summit that reflects the heterogeneity in the distribution of peak and valley structures on the membrane surface [30].

3. Results and discussions

3.1. Quantification of dynamic hysteresis

For comparison, a mica sheet was chosen as a standard smooth surface test sheet. Mica sheet is a layered aluminosilicate mineral having one intrinsic negative surface charge per 48 Å and also known for its smooth surface. To test the heterogeneity, the mica sheet was tested with four different RO membranes using the dynamic contact angle analyzer. Fig. 1 shows the values of the tested mica sheet and different membranes. As shown in Fig. 1, dynamic hysteresis value varies significantly with respect to the applied surface. Mica sheet was used as a representative homogeneous surface. It is clearly shown in Fig. 1 that dynamic hysteresis for mica sheet is nearly zero (i.e.,advancing and receding forces are similar), while much greater than zero (i.e., advancing and receding forces are different) for the RO membranes tested. Establishing the mica sheet value as a standard, the four membrane dynamic hysteresis values could be shown in actual values. Based on the results, a standard baseline for the hysteresis can be established.

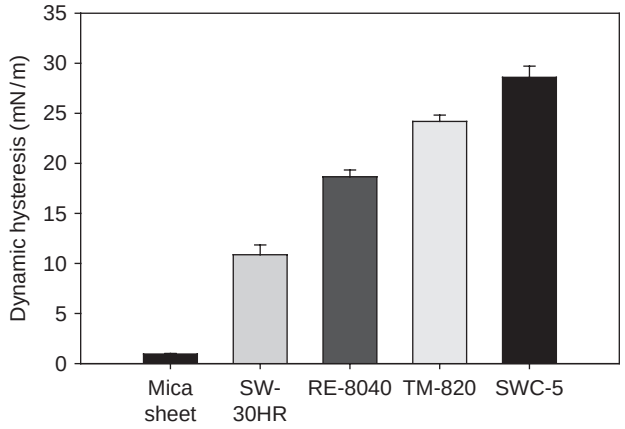

Fig. 1. Quantification of dynamic hysteresis.

3.2. Physical aspects of dynamic hysteresis

3.2.1. Surface roughness and dynamic hysteresis

Surface roughness of the membranes was determined based on AFM imaging and analysis. The RMS roughness values and AFM images of each membrane are shown in Table 1 and Fig. 2, respectively. As listed in Table 1, the RMS roughness was different for each membrane (i.e., SW-30HR > SWC-5 > TM-820 > RE-8040). In addition, as shown in Fig. 2, the distribution of peak and valley structures is also different for each membrane (i.e., morphological surface heterogeneity). Details on the surface heterogeneity and its relation to dynamic hysteresis will be discussed in the following section.

3.2.2. Relationship between the roughness and the dynamic hysteresis

Fig. 3 shows the relation between the RMS roughness and the dynamic hysteresis values. The RMS roughness of the four membranes was determined based on the AFM analysis and also shown in Table 1, respectively. Also dynamic hysteresis values are acquired from Fig. 1 for comparison. As seen in the figure, the SW-30HR membrane shows the highest RMS roughness with the lowest dynamic hysteresis while the RE-8040 membrane shows lower RMS and higher dynamic hysteresis values. Based on these results it can be accounted for that there was no substantial correlation between the dynamic hysteresis and the surface roughness. This observation is attributed to the fact that average roughness does not reflect the distribution of peak and valley structures. Therefore, dynamic hysteresis is assumed to be rather related to the morphological surface heterogeneity than the average surface roughness. The verification of this assumption will be made in the following section.

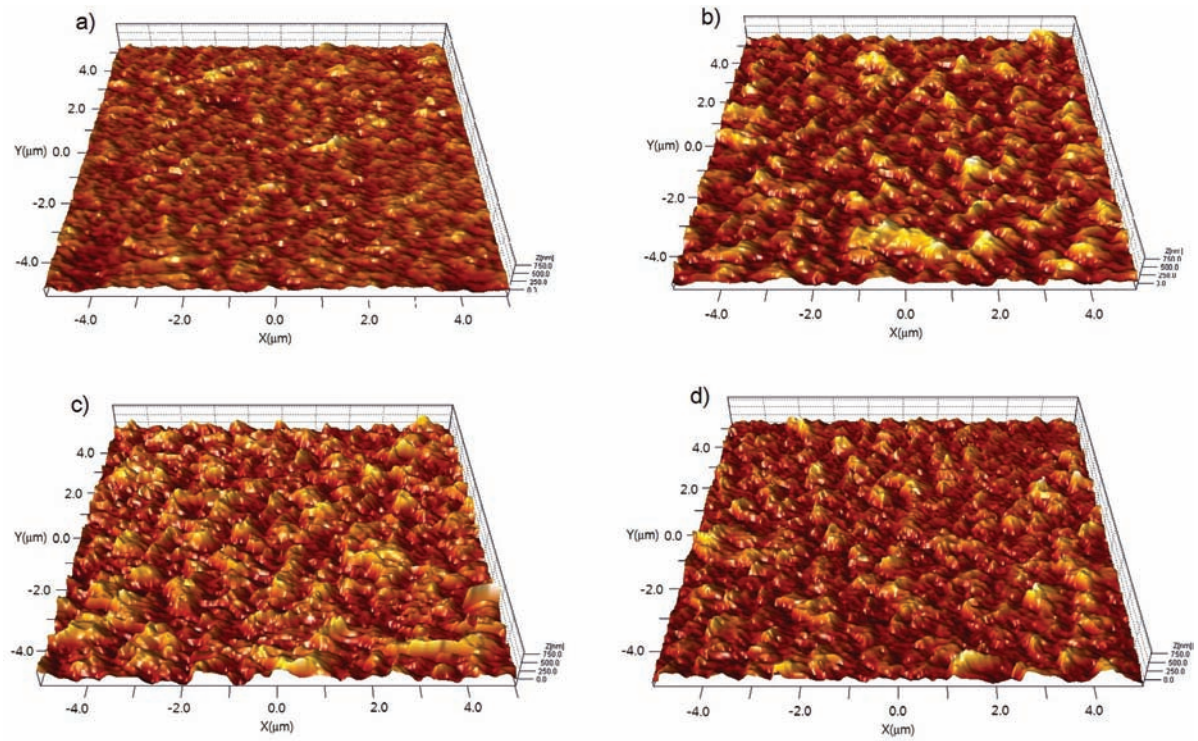

Fig. 2. Liquid phase contact mode AFM images of (a) TM-820, (b) SW-30HR, (c) SWC-5, and (d) RE-8040. Note that the *X* and *Y* dimensions are both 10 μm, while the *Z*-scale is 200 nm

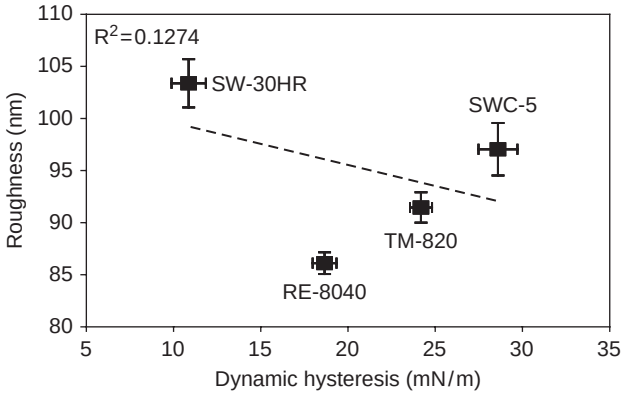

Fig. 3. Correlation between surface roughness and dynamic hysteresis determined using the polar liquid (i.e., water); regression coefficient (R^2) is included.

3.2.3. Surface heterogeneity and dynamic hysteresis

In this study, the density of summit was used as a parameter to show the physical surface heterogeneity. Density of summit is defined as the number of local maximums per unit area where the unit of $1/\mu m^2$ is employed [31]. Therefore, the degree of heterogeneity in the distribution of the peak and valley structures of the membrane surface can be quantified by the density of summit (i.e., the higher the density of summit, the more the heterogeneous surface). The relation between the surface heterogeneity and the dynamic hysteresis for each membrane is shown in Fig. 4. If the surface is uniform in roughness as the figure on the left, the advancing and receding forces will be equal making an even force hysteresis. When the surface has a non-uniform distribution of peak and valley structure, force hysteresis is induced during the dynamic movements at the liquid-solid interface as shown in Fig. 4. So it may be noted that the surface heterogeneity for each membrane does not correspond to the surface roughness (i.e., TM 820 was the highest in the density of summit but the lowest in the surface roughness). Fig. 5 shows the relation between the dynamic hysteresis and the surface heterogeneity. Here it can be seen that the dynamic hysteresis is loosely related to the morphologial heterogeneity of the membrane surface compared to the relations with the average roughness in Fig. 3.

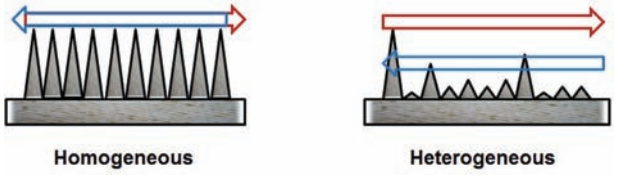

Fig. 4. Schematic illustration of the relationship between dynamic hysteresis and surface heterogeneity.

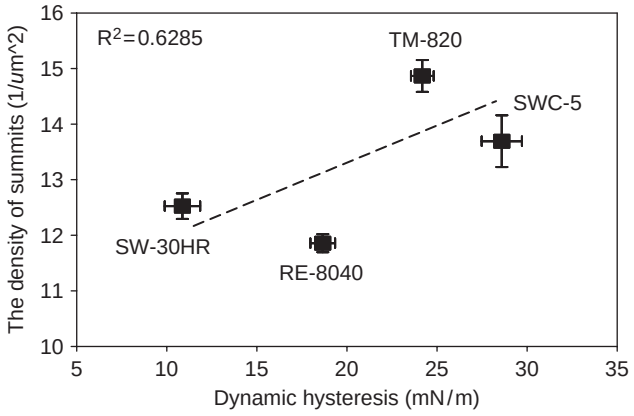

Fig. 5. Correlation between surface heterogeneity (the density of summits) and dynamic hysteresis determined using the polar liquid (i.e., water); regression coefficient (R^2) is included.

The non-polar liquid was used during the measurements. A remarkable correlation was obtained between the surface heterogeneity and the dynamic hysteresis for the membranes investigated. The dynamic hysteresis increased as the surface heterogeneity increased. This implies that non-uniform distribution of peak and valley structures on the membrane surface causes the force hysteresis during the dynamic movements in the liquid–solid interface. Therefore, the dynamic hysteresis can be a reliable parameter in determining the morphological heterogeneity of the membrane surface. It may be noted that the surface heterogeneity for each membrane does not correspond to the surface roughness (i.e., TM 820 was the highest in the density of summit but the lowest in the surface roughness). This also explains the poor correlation between the surface roughness and the dynamic hysteresis observed in the previous section.

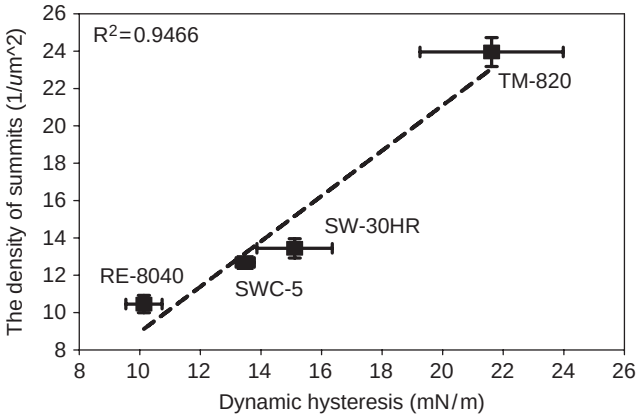

Fig. 6. Correlation between surface heterogeneity and dynamic hysteresis determined using the non-polar liquid (i.e., diiodomethane); regression coefficient (R^2) is included.

The results obtained above showed that the physical surface characteristics of RO membranes could be investigated by dynamic hysteresis with employing non-polar liquid during the measurements. In the concrete, dynamic hysteresis was related to physical surface heterogeneity (i.e., the density of summit), where the non-polar liquid was used to minimize the interference by chemical surface characteristics in Fig. 6. To see how the chemical surface characteristics affect the physical surface characteristics, the interference of chemical surface characteristics with physical surface characteristics was minimized during the measurements as shown in Fig. 6.

4. Conclusion

A systematic investigation on the use of dynamic hysteresis for characterizing RO membranes was performed. Emphasis was placed on physical aspects of dynamic hysteresis. Surface characteristics of four commercial TFC RO membranes were investigated focusing on physical (i.e., surface roughness and heterogeneity) characteristics. Measurements of dynamic hysteresis were carried out with two different test liquids (i.e., polar and non-polar). It was shown that dynamic hysteresis could be used as a parameter of showing both chemical and physical surface characteristics of RO membranes investigated. Dynamic hysteresis determined using the non-polar liquid was remarkably related to the physical surface characteristics (i.e., morphological surface heterogeneity). For the membranes investigated, the membrane with higher surface heterogeneity exhibited the higher dynamic hysteresis. The results from this study suggest that dynamic hysteresis can be a simple and reliable tool for characterizing physical surface characteristics of RO membranes.

Acknowledgment

The authors thank the Ministry of Land, Transport and Maritime Affairs (MLTM) for supporting this study through Seawater Engineering & Architecture of High Efficiency Reverse Osmosis (SEAHERO) program.

References

[1] C. Jucker and M.M. Clark, Adsorption of aquatic humic substances on hydrophobic ultrafiltration membranes, J. Membr. Sci., 97 (1994) 37–52.
[2] A.E. Childress and M. Elimelech, Effect of solution chemistry on the surface charge of polymeric reverse osmosis and nanofiltration membranes, J. Membr. Sci., 119 (1996) 253–268.
[3] C.-C. Ho and A.L. Zydney, Effect of membrane morphology on the initial rate of protein fouling during microfiltration, J. Membr. Sci., 155 (1999) 261–275.
[4] Y. Shim, H.J. Lee, S. Lee, S.H. Moon and J. Cho, Effects of natural organic matter and ionic species on membrane surface charge, Environ. Sci. Technol., 36 (2002) 3864–3871.
[5] S. Al-Jeshi and A. Neville, An investigation into the relationship between flux and roughness on RO membranes using scanning probe microscopy, Desalination, 189 (2006) 221–228.
[6] S. Lee and M. Elimelech, Relating organic fouling of reverse osmosis membranes to intermolecular adhesion forces, Environ. Sci. Technol., 40 (2006) 980–987.
[7] K. Boussu, A. Belpaire, A. Volodin, C. Van Haesendonck, P. Van der Meeren, C. Vandecasteele and B. Van der Bruggen, Influence of membrane and colloid characteristics on fouling of nanofiltration membranes, J. Membr. Sci., 280 (2007) 220–230.
[8] J. Pieracci, J.V. Crivello and G. Belfort, Photochemical modification of 10 kDa polyethersulfone ultrafiltration membranes for reduction of biofouling, J. Membr. Sci., 156 (1999) 223–240.
[9] V. Freger, J. Gilron and S. Belfer, TFC polyamide membranes modified by grafting of hydrophilic polymers: an FT-IR/AFM/TEM study, J. Membr. Sci., 209 (2002) 283–292.
[10] S. Belfer, R. Fainshtain, Y. Purinson, J. Gilron, M. Nyström and M. Mänttäri, Modification of NF membrane properties by in situ redox initiated graft polymerization with hydrophilic monomers, J. Membr. Sci., 239 (2004) 55–64.
[11] L.-F. Liu, S.-C. Yu, Y. Zhou and C.-J. Gao, Study on a novel polyamide-urea reverse osmosis composite membrane (ICIC–MPD): I. Preparation and characterization of ICIC–MPD membrane, J. Membr. Sci., 281 (2006) 88–94.
[12] B.J.A. Tarboush, D. Rana, T. Matsuura, H.A. Arafat and R.M. Narbaitz, Preparation of thin-film-composite polyamide membranes for desalination using novel hydrophilic surface modifying macromolecules, J. Membr. Sci., 325 (2008) 166–175.
[13] J.-H. Li, Y.-Y. Xu, L.-P. Zhu, J.-H. Wang and C.-H. Du, Fabrication and characterization of a novel TiO2 nanoparticle self-assembly membrane with improved fouling resistance, J. Membr. Sci., 326 (2009) 659–666.
[14] J. Yang, S. Lee, E. Lee, J. Lee and S.K. Hong, Effect of solution chemistry on the surface property of reverse osmosis membranes under seawater conditions, Desalination, 247 (2009) 148–161.
[15] A.E. Childress and S.S. Deshmukh, Effect of humic substances and anionic surfactants on the surface charge and performance of reverse osmosis membranes, Desalination, 118 (1998) 167–174.
[16] E.M.V. Hoek, S. Bhattacharjee and M. Elimelech, Effect of membrane surface roughness on colloid-membrane DLVO interactions, Langmuir, 19 (2003) 4836–4847.
[17] J.A. Brant, K.M. Johnson and A.E. Childress, Examining the electrochemical properties of a nanofiltration membrane with atomic force microscopy, J. Membrane Sci., 276 (2006) 286–294.
[18] A.M. Gaudin and T.G. Decker, Contact angles and adsorption in the system quartz water-dodecane modified by dodecyl ammonium chloride, J. Colloid Interface Sci., 24 (1967) 151–158.
[19] Nabe, E. Staude and G. Belfort, Surface modification of polysulfone ultrafiltration membranes and fouling by BSA solutions, J. Membr. Sci., 133 (1997) 57–72.
[20] H. Kamusewitz, W, Possart and D. Paul, The relation between Young's equilibrium contact angle and the hysteresis on rough paraffin wax surfaces, Colloids Surf. A., 156 (1999) 271–279.
[21] F. Rupp, L. Scheideler and J. Geis-Gerstorfer, Effect of heterogenic surfaces on contact angle hysteresis: dynamic contact angle analysis in material sciences, Chem. Eng. Technol., 25 (2002) 9–15.
[22] S.-H. Lee, C.-S. Lee, D.-S. Shin, B.-G. Kim, Y.-S. Lee and Y.-K. Kim, Micro protein patterning using a lift-off process with fluorocarbon thin film, Sens. Actuators. B, 99 (2004) 623–632.
[23] C. Brunot, B. Grosgogeat, C. Picart, C. Lagneau, N. Jaffrezic-Renault and L. Ponsonnet, Response of fibroblast activity and polyelectrolyte multilayer films coating titanium, Dent. Mater., 24 (2008) 1025–1035.
[24] T. Kasemura, S. Takahashi, N. Nakane and T. Maegawa, Surface dynamics for poly (vinyl alkylates) via dynamic contact angle and adhesion tension relaxation, Polymer, 37 (1996) 3659–3664.

[25] Y.-L. Lee, Y.-C. Chen, C.-H. Chang, Y.-M. Yang and J.-R. Maa, Surface characterization of the monolayer and Langmuir–Blodgett films of tetra-tert-butyl-copper phthalocyanine, Thin Solid Films, 370 (2000) 278–284.
[26] A.A. Keller, V. Broje and K. Setty, Effect of advancing velocity and fluid viscosity on the dynamic contact angle of petroleum hydrocarbons, J. Petrol. Sci. Eng., 58 (2007) 201–206.
[27] X. Xie, N.R. Morrow and J.S. Buckley, Contact angle hysteresis and the stability of wetting changes induced by adsorption from crude oil, Journal of Petroleum Science and Engineering, 33 (2002) 147–159.
[28] M. Weikart, M. Miyama and H.K. Yasuda, Surface modification of conventional polymers by depositing plasma ploymers of trimethylsilane and of trimethylsilane+O2, J. Colloid Interface Sci., 211 (1999) 28–38.
[29] A. Marmur, Equilibrium contact angles: theory and measurement, Colloid Surf. A, 116 (1996) 55–61.
[30] K.J. Stout, P.J. Sullivan, W.P. Dong, E. Mainsah, N. Luo, T. Mathia and H. Zahouani, The development of methods for the characterization of roughness on three dimensions. Publication No. EUR 15178 EN, Commission of the European Communities, Luxembourg, 1994.
[31] V. Freger, J. Gilron and S. Belfer, TFC polyamide membranes modified by grafting of hydrophilic polymers: an FT-IR/AFM/TEM study, J. Membr. Sci., 209 (2002) 283–292.